

*Full Length Research Paper*

## **Edge Detection innovator based on wavelet coefficients for images corrupted by the white-gaussian noise**

**Alaa. Kh. Al-Azzawi<sup>1\*</sup>, M. Iqbal Saripan<sup>1</sup>, Adznan Jantan<sup>1</sup>, Rahmita Wirza O. K. Rahmat<sup>2</sup>**

<sup>1</sup>Department of Computer and Communication Systems Engineering, Faculty of Engineering, University Putra Malaysia (UPM), 43400, Serdang, Selangor Darul Ehsan, Malaysia.

<sup>2</sup>Department of Multimedia, Faculty of Computer Science and Information Technology, University Putra Malaysia.

Accepted 31 October, 2011

**Denoising of images is one of the vital topics in image manipulating. Approaches for denoising a chain of images aims to attenuate additive noise to the lowest possible rates by using both spatial and temporal areas. Conversely, extracting the edges of images that affected by the White-Gaussian noise was the major dilemma faced by many researchers. Many of the denoising image methods based on wavelet have been proposed to extract the edges from both the vertical and horizontal image gradients. In this paper, denoising of images obtained after thresholding of wavelet coefficients. At the same time, an adaptive average filtering for each pixel in the neighborhood of the processed pixel is used. The method could denoise each of the smooth piecewise as well as images of the natural textured as they were carried enough redundancy. Furthermore, the weights in this averaging were determined after finding similar patches in the neighborhood around pixels matched to describe their contents. Accordingly, the best extraction method for the vertical and horizontal image gradients is achieved after changing the magnitude of the threshold. These were extracted from the histogram of these gradients. Experiment results demonstrate that the proposed method simultaneously provided significant improvements in terms of the blockiness artifacts as well as enhancing the quality of images in terms of visual perception.**

**Key words:** Image denoising, edge detection (ED), wavelet transforms (WT), image gradients.

### **INTRODUCTION**

Results of experimental studies in image de-noising offered a lot of meaningful applications, for example, extracting the edges, a lossy compression, textures, cessations, and low light imaging. In this paper, we focused on extracting the edges of the blurred images. The challenge was how to choose the best method for extracting these edges. Mathematically, images are otherwise smooth functions with cessations along curves and these cessations along curves are edges. Edges are very necessary in recognizing the images.

Standard wavelet transformations have limited possibilities to solve these directional properties. In the meantime, curvelet transform is used to overcome the limitation capability of the wavelets in the representation of the edges. For clarification, the curvelets are geometric multiscale transform, which are intended for two dimensional functions, used to provide sparse representation of images with singularities along curves, as well as extracting the edges while; wavelets provide the best reconstruction of smooth areas and small patches.

In most cases, image sequences are noisier than singular images due to the high capture proportion. This leads us to the use of temporal dimension, which is most appropriate in dealing with these sequences. The

---

\*Corresponding author. E-mail: [ali\\_ksaleh2010@yahoo.com](mailto:ali_ksaleh2010@yahoo.com).  
Tel: 0060172851969.

proposed method in Protter et al. (2009) was the extension to work in each of Elad et al. (2006a and b). This method provided sparse and redundant representation to de-noising image sequences corrupted by the White-Gaussian noise. While, in the singular images, the method of clustering singular value decomposition (K-SVD), which is presented in each of Aharon et al. (2006a and b) had been used to coach a sparsifying dictionary for the corrupted image, assuming that each patch in the image has a sparse representation describes the content. Whereas in the maximum a posteriori probability (MAP) framework, the methods proposed in each of Elad et al. (2006a and b) are ideal methods that could deal with applications of the singular de-noising images.

Crouse et al. (1998) explained that the models' eventualities for wavelet coefficients, including Gaussian mixture, Gaussian scale mixture, Portilla (2003), and circular-symmetric Laplacian (Sendur et al., 2002) are adopted in applications.

From another point of view, using the modern wavelet techniques, for example, curvelets, Candes et al. (1999) has greatly helped in creating of many of the changes, this reflected positively in the selection of the best manner to extract the edges of images. On the other hand, statistical modeling of the wavelet can be evaluated heuristically. Hirakawa et al. (2006) suggested a method for removing noise from the digital images that are corrupted by the additive, multiplicative, and mixed noise.

Furthermore, a patch from an ideal image can be modeled as a linear combination of patches of a noisy image. The proposed method in Kervrann et al. (2006) is an adaptive and patch-based of image de-noising and representation. This method is based on a point wise selection of the small image patches of fixed size in the non-invariant neighborhood of each pixel. It also aims to be associated with each pixel the weighted sum of data points within an adaptive neighborhood and can be applied under the assumption that there exist repetitive patterns in a local neighborhood of a point.

Wu et al. (2005) suggested in the selection of an optimal threshold, which selects the de-noising threshold according to the turbulent degree of detected edge points in edge detection based on wavelet transform, in which adjacent domain division algorithm (ADDA) and parabola fitting algorithm (PFA) is used to separate edge curves from each other after wavelet transform. In addition, the entropies corresponding to the possible thresholds can be calculated by the adoption of each of the numbers and lengths of the detected curves.

Several methods had been suggested to study and tackle the problems of extracting edges of images. These methods have been classified into two categories: (1) gradient, and (2) Laplacian. In the gradient method, the edges were detected by looking for maximum and minimum magnitudes in the first derivative of the image.

While in the Laplacian method, inspecting for zero-crossings in the second derivative of the image were utilized.

In this paper, vertical and horizontal image gradients were extracted from the denoising image and then created an appropriate threshold of the histogram of the magnitudes of those gradients. In this context, traditional methods used to remove mitigation of noise and specifically, images corrupted by white-Gaussian noise have been developed through the results of simulations of this paper. The proposed method used each of the sparse and redundant representations of the sequences of the de-noising images. In addition, new adaptive impulse filters to refine the images from the decomposition of "Haar" wavelet is derived.

Subsequently, approximate expressions for the de-noising score and the use of robust estimate was derived and the procedure to obtaining the image gradients and edge detection related to our work explained. A brief description for a perfect matching boundary and numerical solutions to the non-local smoothing filter is also discussed.

## WAVELET THRESHOLDING

Thresholding is a non-linear technique based directly on wavelet coefficients, in which each coefficient was compared with the threshold value. In the case where the value of a coefficient smaller than the threshold, this is required to set the coefficient value equal to zero without impacting the quality of the image. While in the case where the value of a largest coefficient, this means that the coefficient is meaningful and important. For clarification, hard thresholding employed the traditional process for setting the value of the elements those were their absolute values less than the threshold equal to zero. The hard threshold is given:

$$H_{TH} = \begin{cases} H_{TH} & \text{if } |H_{TH}| > t_{TH} \\ 0 & \text{if } |H_{TH}| < t_{TH} \end{cases} \quad (1)$$

Let,  $I$  denote the  $M \times M$  matrix of the original image to be threshold.

Let,  $C$  be the outcome coefficients matrix after utilizing the hard thresholding. Therefore, the thresholding image matrix (for example, smoothed image) can be obtained as follows:

$$I_{TH} = T^{-1} \cdot C \quad (2)$$

Where,  $T^{-1}$  denotes the 2-dimensional matrix of the inverse discrete wavelet transform.

The thresholding score in percentage is given as:

$$TH_s = 100 \times (V_w/V_D)^2 \quad (3)$$

Where,  $D$  denotes the wavelet decomposition structure of the input image  $I$ ,  $V_w$  is the vector-norm of the wavelet decomposition structure of  $I_{TH}$ , and  $V_D$  is the vector-norm of the wavelet decomposition structure of  $I$ . If,  $I$  is one-dimensional signal with orthogonal wavelet,  $TH_s$  is reduced to:

$$TH_s = \frac{100 \times \|I_{TH}\|^2}{\|I\|^2} \quad (4)$$

The underlying model for noising signal is basically as follows:

$$s(n) = I(n) + \sigma e(n) \quad (5)$$

Where, time  $n$  is equally spaced. Suppose that  $e(n)$  is a Gaussian white noise  $N(0,1)$  and the noise level  $\sigma$ , is supposed to be equal to 1. The de-noising objective is to suppress the noise part of the signal  $s$  and to recover  $I$ .

In general, we can ignore the noise level that must be estimated. The detail coefficients such as at level-1 (the fines scale) are essentially noise coefficients with standard deviation equal to  $\sigma$ . The median absolute deviation of the coefficients is a robust estimate of  $\sigma$ . The use of robust estimate is crucial for two reasons. The first reason is if level-1 coefficients contain 1 details, these details are concentrated in a few coefficients. The second reason is to avoid signal end effects, which are pure artifacts due to computations on the edges.

## EDGE DETECTION AND RELATED WORK

Edges of the image are often resulted from sharp cessations in intensity function and for several reasons: (1) different depths of objects within the components of the scene; (2) varying in ratios of lighting of these objects, and; (3) the actual features of these objects. Accordingly, the edges of image and in most cases are attributed to the gradient image, in which the intensity of objects had been presented prominent peaks near the lighting cessations.

Most of the methods used to detect edges of the images were based on multi-stage detectors. These detectors do not deal directly with the details of the image within the different levels of gray but take advantage of intermediate representations. Thus, such detectors, used

some kernels in the spatial domain for the purpose of obtaining filtered images (Haralick, 1984) or performing a match with a predefined edge templates (Shneier, 1982), it will then be to apply some of the operations of the threshold election, which aims to reduce the noisy edge points.

One of the most used approaches in this field is the edge detector proposed by Canny (1986), which was considered a standard of comparison in assessing the efficiency of performance. Grigorescu et al. (2004) used some of the computational applications, which were called by surround suppression to improve detection of objects schemes in natural scenes. These calculations were supported by neural network to distinguish the edges and lines after adding of the Canny edge detector, for the purpose of separating each of the lines and edges respectively.

Ye et al. (2005) proposed edge detection algorithm at sub-pixel level, after the adoption of a model for a corrupted edge. This method was applied to both synthetic and real images for the purpose of assessing after the use of some of derivatives of the least-squared error.

The detection technique in Dong et al. (2005) gave better norm for detecting edge points. This technique combined each of pixel-level method and sub-pixel-level method to detect the target edge. In addition, this detection consisted of two steps: First, all probable edge points were detected utilizing the Sobel operator; secondly, Zernike moments operator was utilized to accurately transport edges from the detected points by Sobel operator, in this step, two masks (one real and one complex) were reduced and based on the Zernike moments theory.

In the meantime, Shih MY, et al. (2005) explained that extraction the edges by using only the image gradients will appear blurring in addition to breaking these edges. Whereas, the proposed method in Hirakawa et al. (2006) aimed to reduce the contributions from the irrelevant image patches as well as reducing the edge artifacts.

From the other point of view, the proposed method in He et al. (2007) exploited efficiently to extract the edges of images corrupted by white-Gaussian noise, and also accurately to locate these edges. More than this, the methods in Belaid et al. (2008), Novotny et al. (2005), and Amstutz et al. (2005) indicated that it is probably to solve the problems of image restoration specifically, edges and gradients of images by using the topological idealization tools. Also, they clarified that image can be viewed as a piece-wise smooth function while, the edges can be considered as set of singularities.

The method in Hermosilla et al. (2008) was non-linear interpolation procedure based on the essentially non-oscillatory (ENO). In this method, there are two cases should be taken into consideration: (1) each pixel of the image represents a point value, and; (2) the pixel is an average value of a function. After image interpolation, the

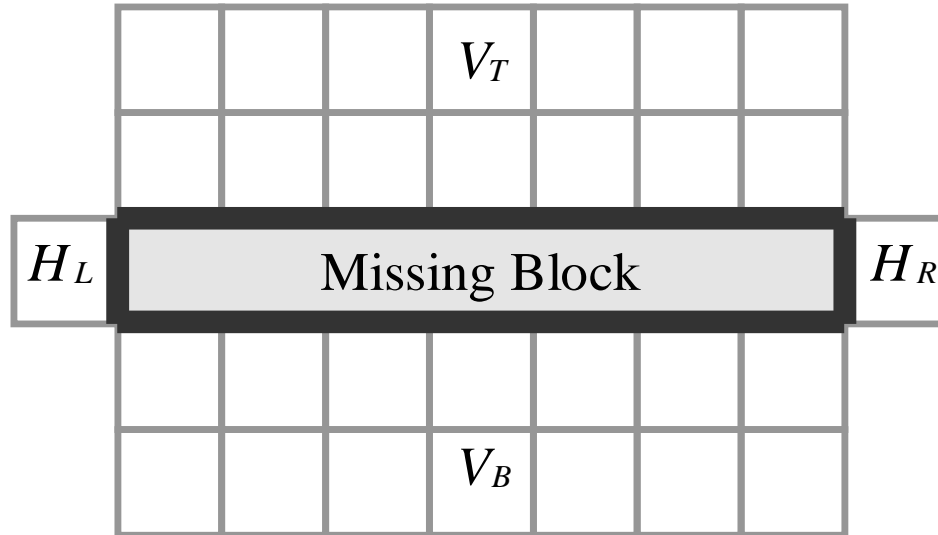


Figure 1. Neighbouring boundary pixels to the corrupted MB.

canny edge detection is applied, with the objective of improving the localization and geometry of the edges at a sub-pixel level.

The method in Carnicer et al. (2008) was a non-parametric method for uni-model thresholding in the context of edge detection. This method assigned a point in a receiver operating characteristic (ROC) space to each possible threshold without the need of a reference image. The goal of the work in Martin et al. (2004) was to accurately detect and localize boundaries in natural images using local image measurements (brightness, color, and texture exemplars).

Zhang et al. (2009) suggested an edge detection method based on directional wavelet transform, which reserves the separable filtering and the simplicity of computations and filter design from the two-dimensional WT, and the image gradients magnitudes is also redefined. While we have seen that the proposed method in Sen et al. (2010) have been carried out on accurate analysis to extract image gradients through an appropriate threshold level taken from image gradient histogram. This threshold is the same as the upper threshold that is used in the hysteresis process for eliciting the edges.

Finally, the method in Coleman et al. (2010) was adaptive procedure for image gradient operators utilized to change the shape to accommodate irregular data distribution, through appropriate analysis of the output responses. This method was most appropriate for direct use on range image data without re-sampling.

In this paper, both gradient magnitude and gradient orientation are expressed in terms of the two directional derivatives  $\partial_v I(i, j)$  and  $\partial_h I(i, j)$ . The gradient magnitude is defined as:

$$|\nabla I(i, j)| = \sqrt{(\partial_v I(i, j))^2 + (\partial_h I(i, j))^2} \quad (6)$$

Where,  $I(i, j)$  is a continuous image,  $i$  and  $j$  are the row and column coordinates, respectively. And the gradient orientation is given as:

$$\theta(i, j) = \tan^{-1}(G_H(i, j)/G_V(i, j)) \quad (7)$$

Where,  $G_H, G_V$  are the horizontal and vertical image gradients. Further, the threshold has been extracted from the histograms of the magnitudes of the gradients. This procedure greatly facilitates the evaluation of the desired results in the detection of the edges. Furthermore, the edge components in the neighboring boundary pixels, which are surrounded with the group of damaged blocks, are detected. Therefore, and for every block in the damaged group, it is an indication to decide whether any of these edges has an impact on the block. At the same time, each pixel in this damaged block is interpolated with the boundary pixels according to the corresponding edges.

The method of the quadrilinear border interpolation (QBI) interpolates the value of the missing pixel ( $M_P$ ) in the damaged block, as shown below, as shown in Figure 1.

Where,  $V_T, V_B, H_L, H_R$  are the vertical top, bottom, and horizontal left, right pixels, respectively.

$$M_P = \frac{P_T \cdot D_B + P_B \cdot D_T + P_L \cdot D_R + P_R \cdot D_L}{D_B + D_T + D_R + D_L} \quad (8)$$

Where,  $P_T, P_B, P_L,$  and  $P_R$  are the top, bottom, left, and right pixels. And  $D$  is the distance between the missing pixel  $M_P$  and four adjacent pixels.

In the case where the LB has one dominate edge, perhaps only two of LB\_HT, LB\_HB, LB\_HR, LB\_HL is small. The missing pixel  $M_P$  is obtained from.

$$M_P = \frac{D_B \cdot P_T}{D_T + D_B} + \frac{D_T \cdot P_B}{D_T + D_B} \quad (9)$$

While in the case where the edge is smooth (that is, object is out of focus). There are two trends of the solution to detect such edges. One is to use the CvT instead of WT, which is only good at isolating the discontinuities at edge points, but cannot detect the smoothness along the edges, and the other is to combine the original images' edge with the filtered image in each subband. If we were to classify a block containing an edge as texture, it requires us to consider the 8-neighborhood of a  $8 \times 8$  block and calculate the difference between the average values of the blocks on opposite sides of the center block. If the 4 resulting differences are below a threshold, this is an indication that an edge does indeed pass through the textured block.

On the other hand, blocking artifacts are generated by independent coding of adjacent groups of pixels and are typically represented by unexpected transitions of luminance across block boundaries. This leads in decreasing the smoothness of image data. Let  $O$  and  $D$  represent the vectors of original image and distorted image from blocking artifacts, respectively. Let  $e$  be the vector of error between  $O$  and  $D$ .

If, the number of pixels in an image is  $N$ , then:

$$\begin{aligned} MSE(O, D) &= \frac{1}{N} \sum_{i=1}^N e_i^2 \\ &= \frac{1}{N} \sum_{i=1}^N (O_i - D_i)^2 \end{aligned} \quad (10)$$

The structural similarity (SSIM) metric aims to measure quality by capturing the similarity of image. The structure comparison function  $S(O, D)$  is defined as:

$$S(O, D) = \frac{\sigma_{OD} + C}{\sigma_O \sigma_D + C} \quad (11)$$

Where  $\sigma_{OD}$  is the correlation between  $O$  and  $D$  and  $C$  is a constant that provides stability. The amount of

compression and the quality can be controlled by the quantization step. As the quantization step size becomes larger, the structural differences between original and distorted image will generally increase, and in particular the structure term  $S(O, D)$  will become smaller. Finally, the proposed method can miss a true edge in the case where the luminance comparison function  $L(O, D)$  is used in order to control the smoothness of image data and given as:

$$L(O, D) = \frac{2\mu_O \mu_D + C}{\mu_O^2 + \mu_D^2 + C} \quad (12)$$

Where  $\mu_O$  and  $\mu_D$  are the mean values of  $O$  and  $D$ , respectively.

## MATERIALS AND METHODS

### Image denoising

Denoising of images is one of the vital topics in image manipulating. In image applications over unreliable channels, the decoder has to contend with data corrupted by channel errors. These errors lead to missing rectangular regions, which needs to be perfectly estimated by appropriate recovery and concealment algorithms. In the case where the missing regions of pixels are containing textures, edges, and other image features that are not readily handled by these algorithms. It, therefore, necessitated using denoising rather than EC algorithms. Moreover, the denoising does not require any complex predisposing, segmentation, or edge detection steps, and it can be written as a sequence of denoising operations. In this case, the missing information is likely recovered under the MSE fidelity metric using the sparsity constraint that a portion of the images transforms coefficients over missing regions are zero or close to zero.

In the meantime, if a linear transforms that is expected to provide sparse decompositions over missing regions is used. These small magnitude coefficients can be adaptively determined through thresholding, establish sparsity constraints, and estimate missing regions in images using information surrounding these regions.

In this work, chains of denoising images aim to attenuate additive noise to the lowest possible rate by using both spatial and temporal areas, after thresholding of wavelet coefficients are simulated. At the same time, approaches to extract the edges of images corrupted by the White-Gaussian noise are also extracted. The denoising of images is obtained after the adoption of three steps: 1) computation of wavelet decomposition, 2) thresholding the coefficients of each decomposed level, and 3) computation of wavelet reconstruction. Figure 2 shows the steps required for denoising the images.

The decomposition of a two-dimensional noisy image is accomplished using the wavelet analysis function (i.e., Haar wavelet decomposition). The Haar function decomposed the image of the matrix  $I$  at level  $N$ . The outputs are the decomposition vector  $C$  and the corresponding book-keeping matrix  $S$ .  $N$  should be a strictly positive integer. The decomposition filters are given as:

$$[C \quad S] = Haar(I, N, Lo\_D, Hi\_D)$$

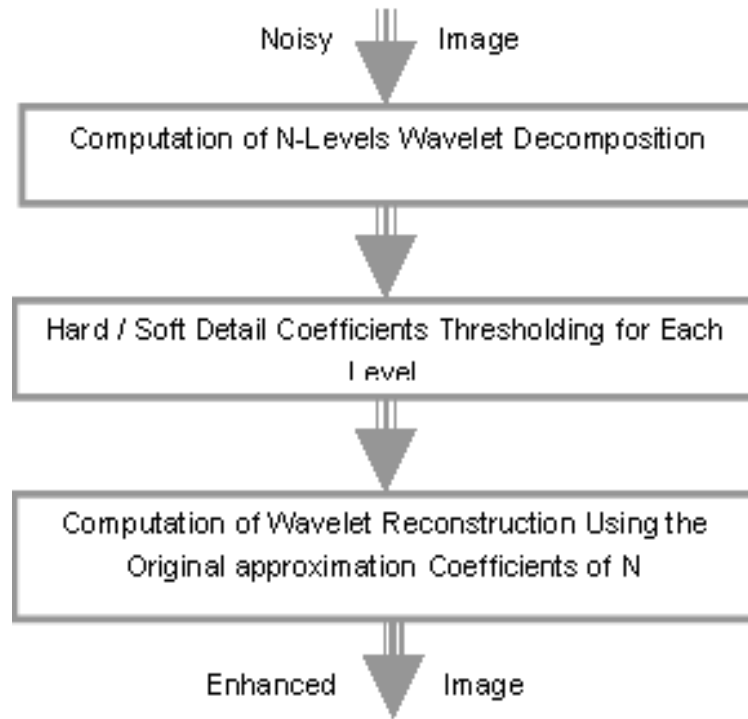


**Figure 2.** The steps required for denoising a two dimensional images.

Where,  $Lo\_D$  and  $Hi\_D$  are the high-pass and low-pass decomposition filters. Vector  $C$  is organized as:

$$C = \begin{bmatrix} A(N) | H(N) | V(N) | D(N) | \dots | H(N-1) \\ | V(N-1) | D(N-1) | \dots | H(1) | V(1) | D(1) \end{bmatrix}$$

where,  $A, H, V$ , and  $D$  are row vectors such that:  $A$  is the approximation coefficients.  $H$  is the horizontal detail coefficients.  $V$  is the vertical detail coefficients, and  $D$  is the diagonal detail coefficients. Matrix  $S$  is such that:  $S(1,:)$  is the size of approximation coefficients ( $N$ ) and  $S(i,:)$ , is the size of detail coefficients ( $N-i+2$ ) for  $i=2, \dots, N+1$  and  $S(N+2,:) = size(I)$ . Figure 3 illustrates the decomposition of the aforementioned analysis.

The denoising procedure which previously mentioned in Figure 2 proceeds in three steps, and uses two-dimensional wavelet tools. Thresholding selection rules are based on the underlying model  $y = I(t) + e$ . Where,  $I$  is a two-dimensional image, and we assume the noise  $e$  to be a white, zero-mean Gaussian noise where,  $e \sim N \{0, \sigma^2\}$ . Dealing with unscaled or nonwhite noise can be handled using a rescaling output threshold. A direct translation of a one-dimensional model is given as:

$$I_n(i, j) = I(i, j) + \sigma e(i, j) \quad (13)$$

Where,  $I_n$  is a noisy image results from noise  $e$  superimposed on an original image  $I$ . In this simulation, the threshold is estimated by the adoption of the following steps:

1. Using a fixed-form threshold yielding mini-max performance multiplied by a small factor proportional to  $\log(\text{length}(I))$ .

The mini-max principle is used in order to design the estimator. The estimator used is MAD ( $\sigma = MAD/0.6745$ ), which is suitable for zero mean Gaussian white noise in the denoising one-dimensional or two-dimensional models.

### Two dimensional adaptive noise removal filtering

The low-pass Wiener filtering is utilized for filtering a grayscale image that has been degraded by constant power additive noise, in which the adaptive pixel wise is based on statistics estimated from the local neighborhood of each pixel is used. The adaptive filter is more selective than a comparable linear filter, preserving edges and other high-frequency parts of an image. The novelty of our proposed filter is in employing an adaptive average filtering for each pixel in the neighborhood of the processed pixel, with the intention of attenuating the noise. Further, the weights in this averaging are determined after finding similar patches in the neighborhood around pixels matched to describe their contents.

In other words, the noisy image  $I_n$  is filtered using pixel wise adaptive Wiener filtering, using neighborhood of size  $M-by-N$  to estimate the local image mean and standard deviation. The estimation of the local mean and variance around each pixel is

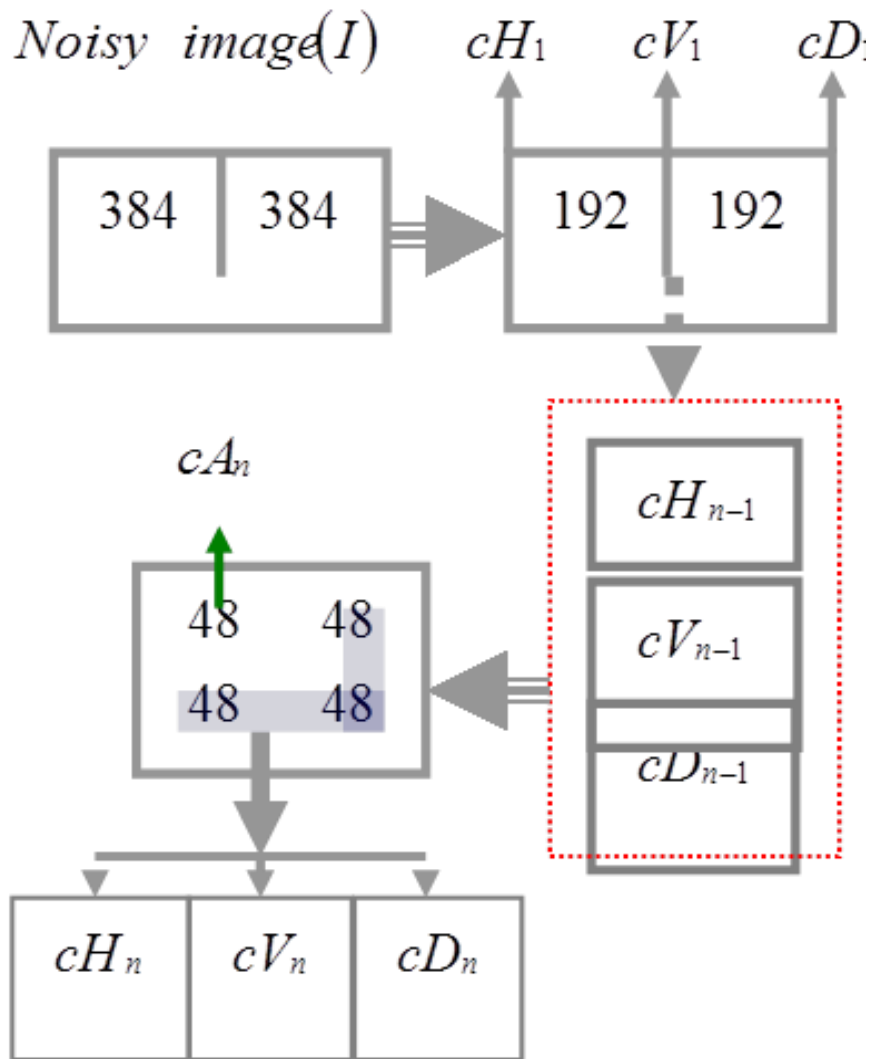


Figure 3. The decomposition analysis of an image with 384 x 384 pixels.

given as:

$$\mu = \frac{1}{MN} \sum_{m_1, n_2 \in \eta} I(n_1, n_2) \tag{14}$$

Where,  $\mu$ , is the local mean, and  $I$  denote the entrance image matrix.

$$\sigma^2 = \frac{1}{MN} \sum_{m_1, n_2 \in \eta} I^2(n_1, n_2) - \mu^2 \tag{15}$$

Where,  $\eta$  is the  $M - by - N$  local neighborhood of each pixel in the image  $I$ .  $\sigma$  is the standard deviation of the zero mean Gaussian white noise in the denoising model. The creation of a pixelwise is achieved after using these estimates:

$$I(n_1, n_2)_{pixelwise} = \mu + \frac{\sigma^2 - v^2}{\sigma^2} \times (I(n_1, n_2) - \mu) \tag{16}$$

Where,  $v^2$  is the noise variance. In the case where the noise variance is not given, Wiener filter uses the average of all the local estimated variances.

**Local Smoothing Process**

The main goal behind the process of local smoothing is to attenuate the noise as well as recover the main geometric disposition but not at the expense of keeping the fine structure and the details. The novelty of our proposed local smoothing is in using sparse and

redundant representations for image sequence denoising. Furthermore, we assume that small image patches in the neighborhood of an estimation pixel contain the essential process required for local denoising. For clarity, the pixel content with a similar patch to the central patch has larger weights in the average. In the gray level images,  $P$  is a point on a two-dimensional grid. Therefore, each pair  $(p, u(p))$ , where  $u(p)$  the value at grid is called a pixel. In this case, the neighborhood of  $P$  is predefined as any set of pixels  $J$  in the image looks like a window around  $P$ .

Let  $I_s$  be the noisy image observation predefined on a bounded domain  $\Omega \subset \mathbb{R}^2$ , and let  $v \in \Omega$ . The nonlocal means algorithm estimated the value of  $v$ , as all values of pixels whose Gaussian neighborhood looks like the neighborhood of  $v$ ,

$$NL(I_s)(v) = \frac{1}{C(v)} \int_{\Omega} e^{-\frac{(G_k * |I_s(x+\cdot) - I_s(y+\cdot)|^2)(0)}{h^2}} I_s(y) d(y) \quad (17)$$

Where,  $G_k$  is a Gaussian kernel with standard deviation  $k, h$  acts as a filtering parameter, and

$$C(v) = \int_{\Omega} e^{-\frac{(G_k * |I_s(x+\cdot) - I_s(y+\cdot)|^2)(0)}{h^2}} d(z), \text{ is the: normalizing factor. We recall that:}$$

$$(G_k * |I_s(x+\cdot) - I_s(y+\cdot)|^2)(0) = \int_{\mathbb{R}^2} G_k(t) |I_s(x+t) - I_s(y+t)|^2 dt.$$

### Denoising simulation and results

The problem with image restoration is to reduce undesirable distortions and noise while preserving important features, such as edges, and textures. Further, the local variance is actually useful for localization of significant image features. From another point of view, natural images often contain many irrelevant objects, thus making image denoising very hard. We have applied the assumption that small image patches in the neighborhood of an estimation point contain the essential process required for local denoising to many standard test images, including, Barbara, cameraman, Lena, and Mandrill.

To obtain results with high accuracy compared with the other conventional methods, our approach to detect the edges of images that are affected by the White-Gaussian noise has been adopted to these sequences, as a criterion for comparison. Here, the threshold extracted from the histogram of the image gradients' magnitudes, this greatly facilitated in extracting the largest number of edges. The calculations of PSNR on the signal impeding capacity of the restoration algorithm and is defined as

follows:  $PSNR = 10 \log_{10} \frac{255^2}{MSE} (dB)$ , where the  $MSE$  between the filtered image,  $U$  and the original noise free image,  $I_n$  of size  $m \times n$  is given as:

$$MSE = \frac{1}{m \times n} \sum_{i=1}^m |U(i_1, i_2) - I_n(i_1, i_2)|^2.$$

Figure 4 shows the vertical and horizontal noisy image gradients, in addition to the histograms of these gradients. To assess the performance efficiency of this method, we have to blur the sequences with the largest possible extent of noise. The relationship between different extents of the White-Gaussian noise and computations of each of MSEs and PSNRs are summarized in Tables 1 and 2, respectively. The results summarized in these Tables are considered as the results of detection of the gradients of sequence images that were placed under test. In this test, the histogram of the image gradients was changed several times after the adoption of different angles to those gradients. The goal behind this work was to extract the largest number of significant edges. The performance efficiency of the proposed method is shown by the simulation sketches shown in the following Figures 5 to 7. While, Figure 8 explains the simulation of each of the denoising and the filtering images for the proposed method.

### CONCLUSION

In this paper, denoising images were successfully obtained through the thresholding of wavelet coefficients. The method could denoise each of smooth piecewise as well as images of the natural textured as they were carried enough redundancy. The novelty of the proposed filter is in employing an adaptive average filtering for each pixel in the neighborhood of the processed pixel, to attenuate the noise to the lowest possible rates. Further, the weights in this averaging were determined after finding similar patches in the neighborhood around pixels matched to describe their contents. Accordingly, the best extraction method for the vertical and horizontal image gradients is achieved after changing the magnitude of the threshold. These were extracted from the histogram of these gradients. Experiment results demonstrated that the proposed method simultaneously provided significant improvements in terms of both blockiness and blurring artifacts, as well as, enhancing the quality of images in terms of visual perception.

### ACKNOWLEDGEMENTS

The authors wish to thank and appreciate all staffs of the Computer and Communication Engineering Department,

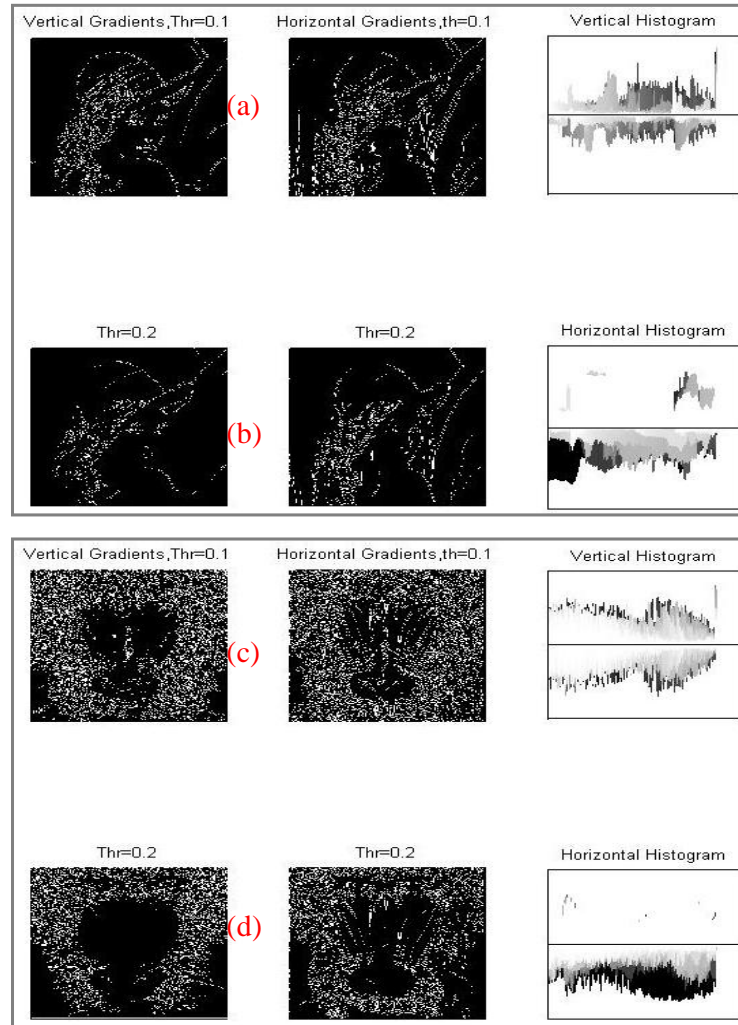


**Figure 4.** The vertical and horizontal noisy image gradients: (a) Threshold = 0.1; (b) Threshold = 0.2; (c) Threshold = 0.3; and (d)Threshold = 0.4.

**Table 1.** The relationship between different extents of the White-Gaussian noise and the computations of MSE for both vertical and horizontal image gradients.

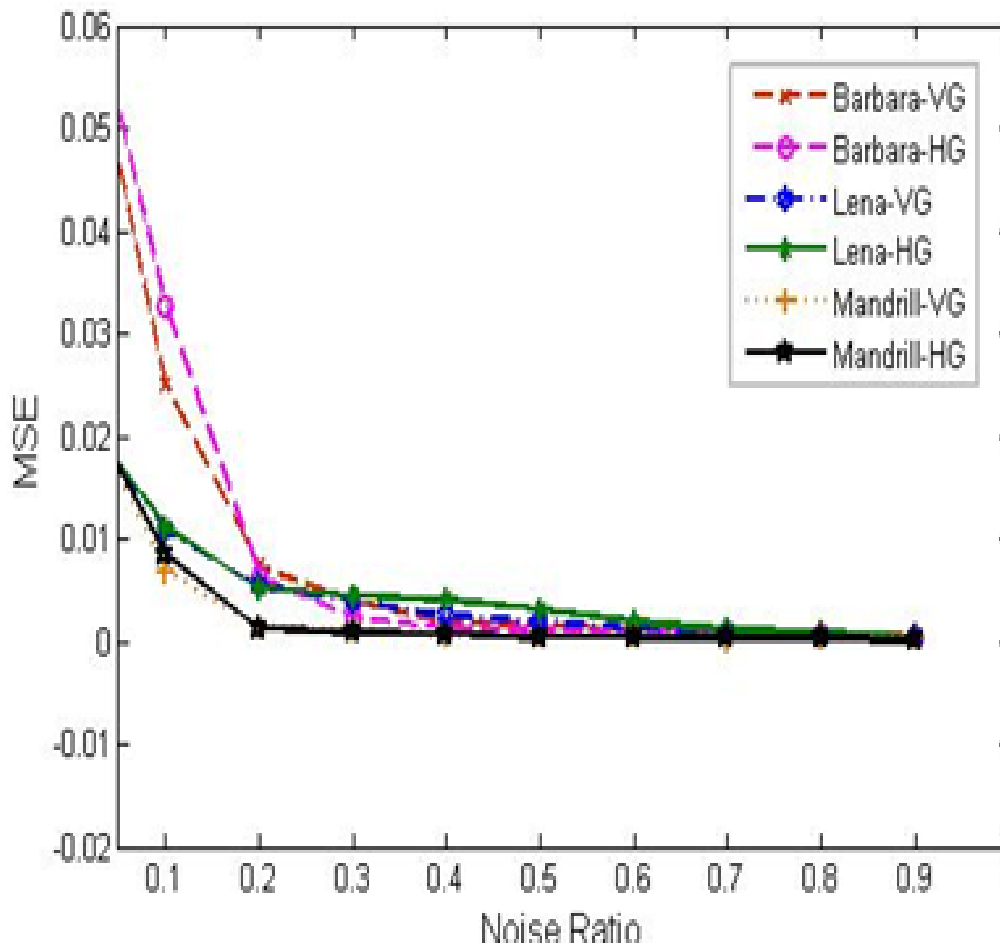
Variable	Ratio	0.0	0.1	0.2	0.3	0.4
Barbara	MSE-VG	0.068	0.025	0.007	0.004	0.001
	MSE-HG	0.070	0.032	0.006	0.002	0.001
Lena	MSE-VG	0.023	0.010	0.005	0.004	0.002
	MSE-HG	0.023	0.011	0.005	0.004	0.004
Mandrill	MSE-VG	0.025	0.006	0.001	0.001	0.000
	MSE-HG	0.025	0.008	0.001	0.000	0.000
	<b>Ratio</b>	<b>0.5</b>	<b>0.6</b>	<b>0.7</b>	<b>0.8</b>	<b>0.9</b>
Barbara	MSE-VG	0.001	0.001	0.001	0.000	0.000
	MSE-HG	0.001	0.001	0.001	0.000	0.000
Lena	MSE-VG	0.001	0.001	0.000	0.000	0.000
	MSE-HG	0.003	0.001	0.001	0.000	0.000
Mandrill	MSE-VG	0.000	0.000	0.000	0.000	0.000
	MSE-HG	0.000	0.000	0.000	0.000	0.000

**Table 2.** The relationship between different extents of the White-Gaussian noise and the computations of the PSNR for both vertical and horizontal image gradients.

Variable	Ratio	0.0	0.1	0.2	0.3	0.4
Barbara	PSNR-VG	29.83	30.83	32.06	32.66	33.40
	PSNR-HG	29.79	30.56	32.21	33.20	33.82
Lena	PSNR-VG	30.91	31.68	32.37	32.67	33.13
	PSNR-HG	30.89	31.64	32.40	32.55	32.65
Mandrill	PSNR-VG	30.83	32.13	33.69	34.00	34.49
	PSNR-HG	30.82	31.91	33.91	34.27	34.34

Variable	Ratio	0.5	0.6	0.7	0.8	0.9
Barbara	PSNR-VG	33.65	33.82	34.01	34.35	34.50
	PSNR-HG	34.00	34.07	34.07	34.62	34.77
Lena	PSNR-VG	33.42	33.80	34.23	35.18	35.18
	PSNR-HG	32.88	33.43	34.00	34.26	35.37
Mandrill	PSNR-VG	34.55	34.55	35.39	35.24	35.24
	PSNR-HG	35.05	35.05	35.05	35.16	36.81



**Figure 5.** The computations of MSE against noise ratios for Barbara, Lena, and Mandrill images' sequences.

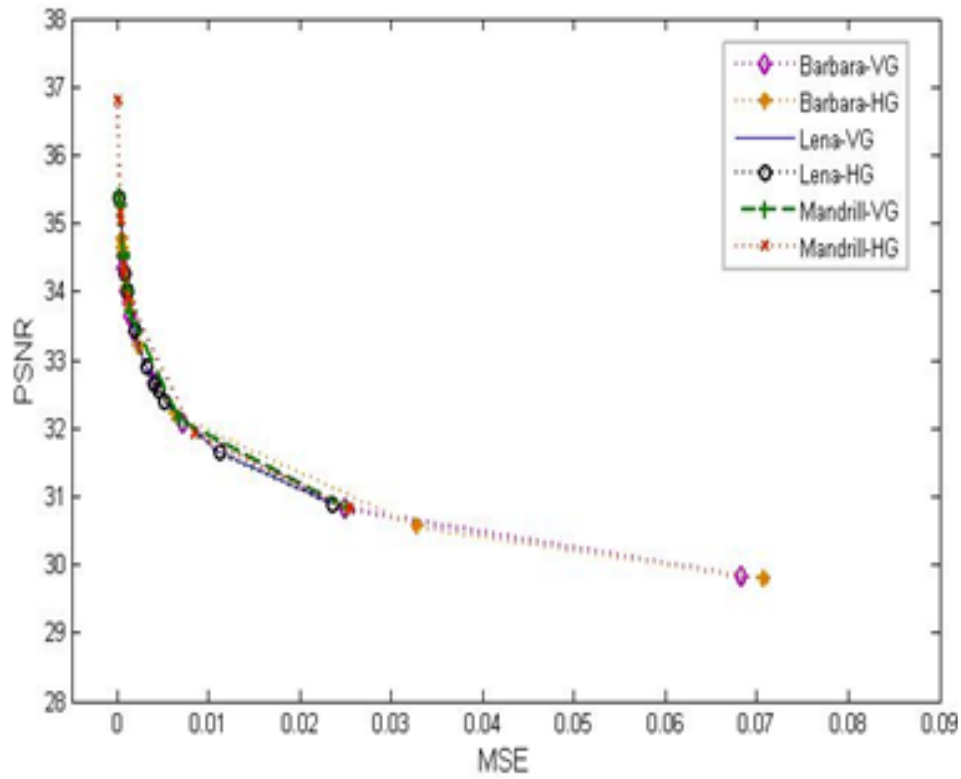


Figure 6. The computations of PSNR against noise ratios for Barbara, Lena, and Mandrill images' sequences.

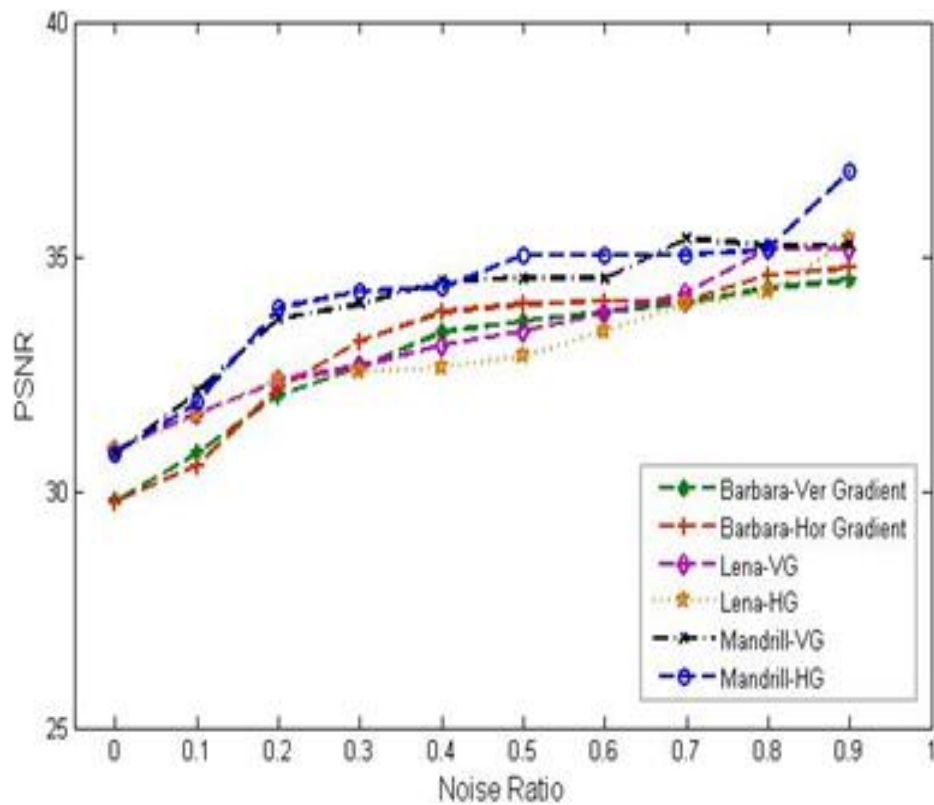


Figure 7. The performance efficiency of the proposed method.

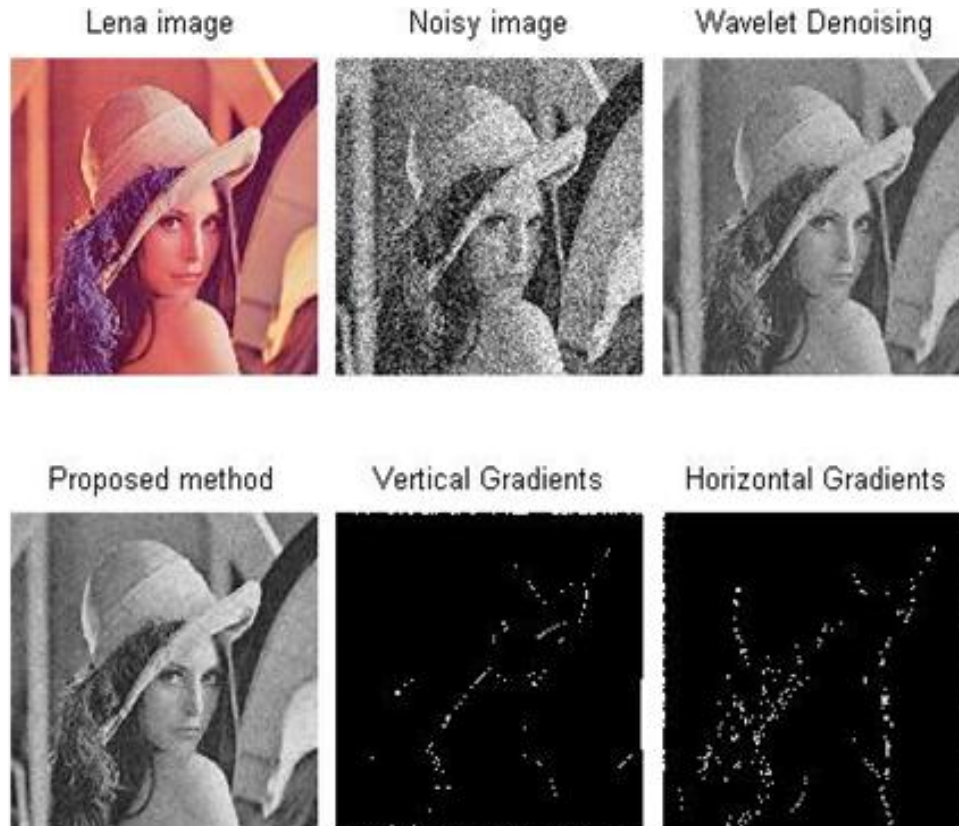


Figure 8. (a) 20% noise.

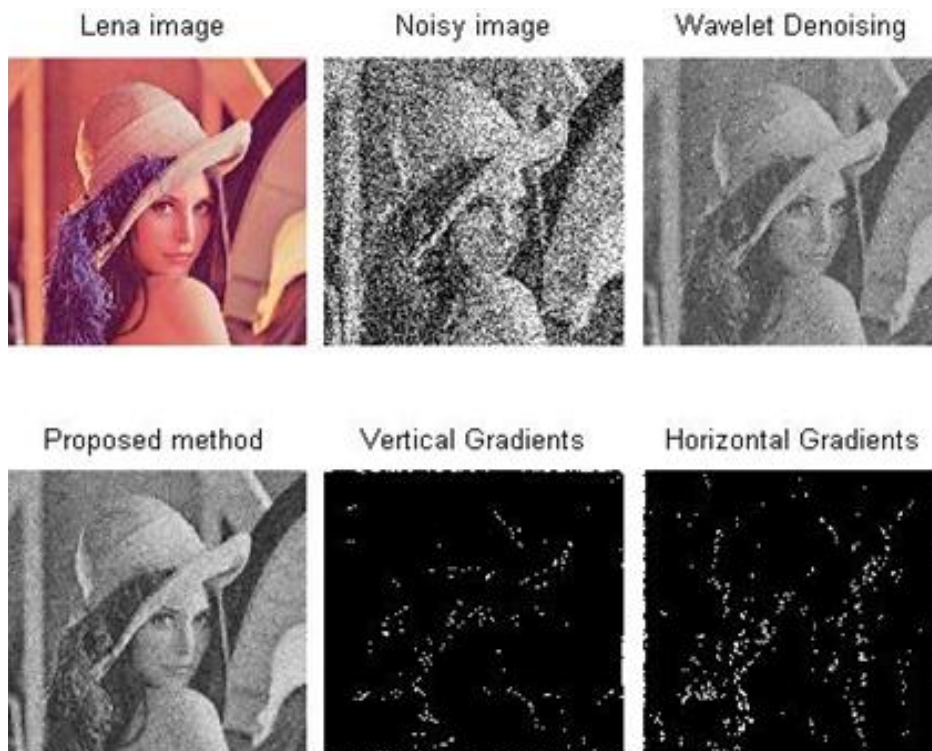


Figure 8. (b) 60% noise.

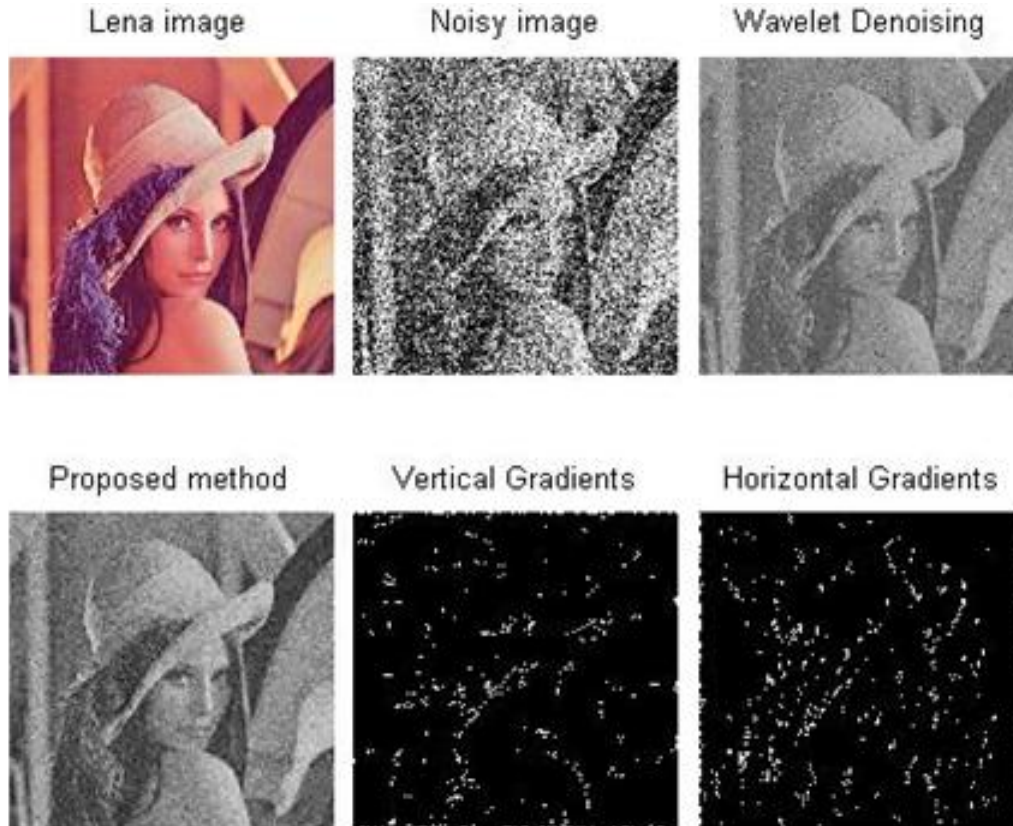


Figure 8. (c) 100% noise.

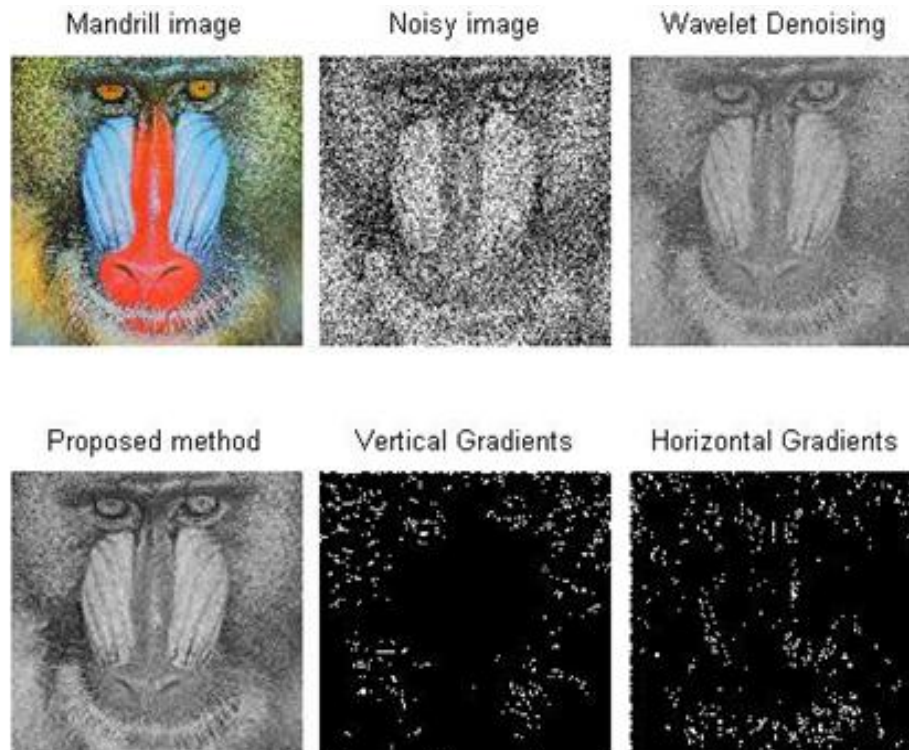


Figure 8. (d) 60% noise.

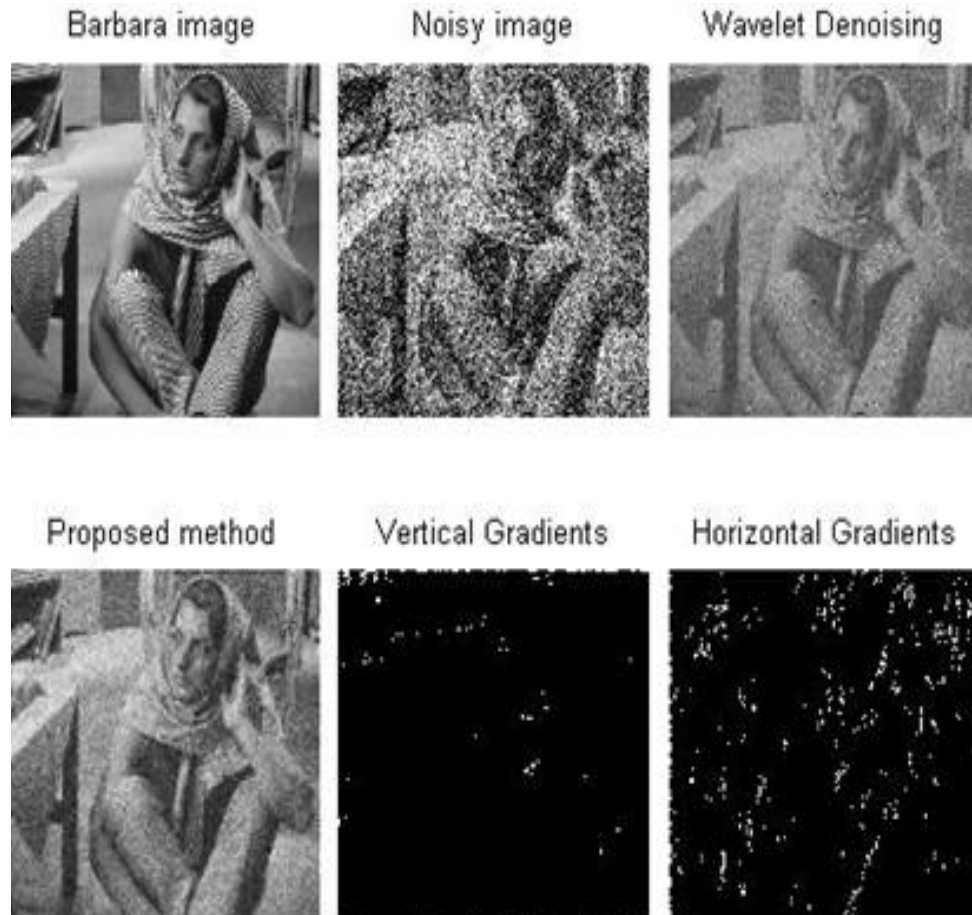


Figure 8. (e) 60% noise.

University Putra Malaysia (UPM), for their support and contributions in the success of this work.

## REFERENCES

- Aharon M, Elad M, Bruckstein AM (2006a). On The Uniqueness of Over-Complete Dictionaries, And A Practical Way To Retrieve Them. *J. Linear Algebra Appl.*, 416(1): 48-67.
- Aharon M, Elad M, Bruckstein AM (2006b). The K-SVD: An Algorithm For Designing of Over-complete Dictionaries For Sparse Representation. *IEEE Trans. Signal Process.*, 54(11): 4311-4322.
- Amstutz S, Horchani I, Masmoudi M (2005). Crack Detection By The Topological Gradient Method. *Control Cybern.*, 34(1): 81-101.
- Belaïd LJ, Jaoua M, Masmoudi M, Siala L (2008). Application Of The Topological Gradient To Image Restoration And Edge Detection. *Eng. Anal. Bound. Elem.*, 32(11): 891-899.
- Crouse MS, Nowak RD, Baraniuk RG (1998). Bayesian Tree-Structured Image Modeling Using Wavelet-Domain Hidden Markov Models. *IEEE Trans. Image Process.*, 46(7): 1056-1068.
- Candes EJ, Donoho DL, Cohen A, Rabut C, Schumaker L, Eds (1999). Curvelets-A Surprisingly Effective Non-Adaptive Representation For Objects With Edges," in *Curve and Surface Fitting*.
- Coleman SA, Suganthan S, Scotney BW (2010). Gradient Operators For Feature Extraction And Characterization In Range Images. *Pattern Recognit. Lett.*, 31(9): 1028-1040.
- Canny J (1986). A Computational Approach To Edge Detection. *IEEE Trans. Pattern Anal. Mach. Intell.*, 8(6): 679-698.
- Carnicer RM, Cueva FJ (2008). Uni-Model Thresholding For Edge Detection. *Pattern Recognit.*, 41: 2337-2346.
- Dong QY, Song CC, Benb CS, Quan LJ (2005). A Fast Subpixel Edge Detection Method Using Sobel-Zernike Moments Operator. *Image Vis. Comput.*, 23(1): 11-17.
- Elad M, Aharon M (2006a). Image Denoising Via Learned Dictionaries and Sparse Representation. *IEEE Int. Con. Comput. Vis. Pattern Recog.*, 1: 895-900.
- Elad M, Aharon M (2006b). Image Denoising Via Sparse and Redundant Representations Over Learned Dictionaries. *IEEE Trans. Image Process.*, 15(12): 3736-3745.
- Grigorescu C, Petkov N, Westenberg MA (2004). Contour And Boundary Detection Improved By Surround Suppression Of Texture Edges. *Image Vis. Comput.*, 22(8): 609-622.
- Hirakawa K, Parks TW (2006). Image Denoising Using Total Least Squares. *IEEE Trans. Image Process.*, 15(9): 2730-2742.
- Haralick RM (1984). Digital Step Edges From Zero Crossing Of Second Directional Derivatives. *IEEE Trans. Pattern Anal. Mach. Intell.*, 6(1): 58-68.
- He Q, Zhang Z (2007). A New Edge Detection Algorithm For Image Corrupted By White-Gaussian Noise. *Int. J. Electron. Commun. (AE-)*, 61(8): 546-550.
- Hermosilla T, Bermejo E, Balaguer A, Ruiz LA (2008). Non-Linear Fourth-Order Image Interpolation For Subpixel Edge Detection And Localization. *Image Vis. Comput.*, 26(9): 1240-1248.
- Kervrann C, Boulanger J (2006). Optimal Spatial Adaptation For Patch-Based Image Denoising. *IEEE Trans. Image Process.*, 15(10): 2866-2878.
- Martin DR, Fowlkes CC, Malik J (2004). Learning to Detect Natural

- Image Boundaries Using Local Brightness, Color, and Texture Cues. *IEEE Trans. Pattern Anal. Mach. Intell.*, 26: 1-20.
- Novotny A, Feijoo R, Padra C, Taroco E (2005). Topological Derivative For Linear Elastic Plane Bending Problems. *Control Cybern.*, 34(1): 339-361.
- Protter M, Elad M (2009). Image Sequence Denoising Via Sparse and Redundant Representations. *IEEE Trans. Image Process.*, 18(1): 27-35.
- Portilla J (2003). Image Denoising Using Scale Mixture of Gaussians in The Wavelet Domain. *IEEE Trans. Image Process.*, 12(11): 1338-1351.
- Sendur L, Selesnick IW (2002). Bivariate Shrinkage Functions For Wavelet-Based Denoising Exploiting Inter-scale Dependency. *IEEE Trans. Signal Process.*, 50(11): 2744-2756.
- Shneier MO (1982). Extracting Linear Features From Images Using Pyramids. *IEEE Trans. Syst. Man Cybernet.*, 12(4): 569-572.
- Sen D, Pal SK (2010). "Gradient Histogram: Thresholding In A Region Of Interest For Edge Detection. *Image Vis. Comput.*, 28(4): 677-695.
- Shih MY, Tseng DC (2005). A Wavelet-Based Multi-Resolution Edge Detection And Tracking. *Image Vis. Comput.*, 23(4): 441-451.
- Wu Y, He Y, Cai H (2005). Optimal Threshold Selection Algorithm In Edge Detection Based on Wavelet Trans. *Image Vis. Comput.*, 23(13): 1159-1169.
- Ye J, Fu G, Poudel UP (2005). High-Accuracy Edge Detection With Blurred Edge Model. *Image Vis. Comput.*, 23(5): 453-467.
- Zhang Z, Ma S, Liu H, Gong Y (2009). An Edge Detection Approach Based On Directional Wavelet Trans. *Comput. Math. Appl.*, 57(8): 1265-1271.